

# Climate Model Capability in Resolving Diurnal Cycle of Rainfall

D. W. Shin, S. Cocke, T. E. LaRow, and Y.-K. Lim

Center for Ocean-Atmospheric Prediction Studies, Florida State University, Tallahassee, FL, USA  
(shin@coaps.fsu.edu)

An investigation is carried out to study the model capability in resolving the diurnal cycle of June-August rainfall using the Florida State University/Center for Ocean-Atmospheric Prediction Studies (FSU/COAPS) climate model (Cocke and LaRow, 2000) and to examine the role of the diurnal cycle in seasonal precipitation simulations. The Tropical Rainfall Measuring Mission multi-satellite precipitation analysis products (TMPA, Huffman et al., 2006) are used as the verification data. In order to uncover which model components are more responsible for the diurnal cycle, a number of seasonal (3-month long) integrations are performed by modifying the climate model configurations.

The observational intensity, in terms of standard deviation, of the diurnal cycle is shown in Fig. 1a. Well-known intense diurnal cycle regions over land can be easily detected. Moderate, but not negligible, diurnal variability is clearly apparent over the ocean, especially along the ITCZ. The corresponding intensities from the five model configurations are illustrated in Fig. 1 as well. While the default FSU/COAPS model with the MIT (Fig. 1f) produces an extremely strong diurnal variability over land, other model configurations generate somewhat weaker diurnal variability compared to the TMPA observation. The diurnal cycle over the oceanic ITCZ is, to some extent, captured only by the NRL at this resolution (T63). Similar intensity maps but for the T255 horizontal resolution are shown in Fig. 2. Although overall results are analogous to the T63 runs, the high resolution runs provide much more detailed diurnal variability and improve the diurnal cycle signal over several regions. In particular, the missed diurnal cycle over the oceanic ITCZ is now somewhat captured even in the CCM3, the NCEP, and the NCAR. Seasonally averaged 3-hourly precipitation evolutions are shown in Fig. 3 in order to assess the phase of precipitation amount from the observation and the models at six selected regions (see Fig. 1a). The five model configurations are the same as those used in Fig. 1. While the late afternoon maxima are clearly shown from the TMPA data over the southeast USA, Indochina Peninsula, and the NAME region, the well-known late night maximum is apparent over the central United States. The diurnal cycle over the ocean exhibits two maxima (the early morning and afternoon) with relatively small magnitude. All of the models produce different phases of diurnal cycle depending on the location. However, the MIT scheme always produces a strong diurnal cycle with the maximum rainfall around the local noon time, regardless of land locations. This implies that the MIT scheme intrigues the most intensive convective activities whenever there is strong incoming solar radiation.

It is found that the convective scheme employed is the most crucial component in properly capturing the diurnal cycle of rainfall. A detailed and improved signal of diurnal cycle is obtained in the experiments with a higher horizontal resolution. A negative influence is found when the Community Land Model version 2 as a land surface scheme is used. No improvement in the oceanic diurnal cycle is discovered even if a frequently coupling ocean model is used rather than prescribed sea surface temperatures. It is also shown that the model configuration which resolves the diurnal cycle better provides an improved seasonal precipitation forecast.

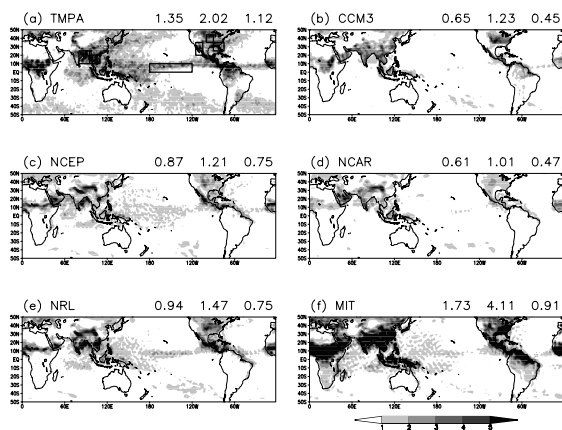


Fig. 1: An observed standard deviation (i.e., intensity,  $\text{mm d}^{-1}$ ) of rainfall diurnal cycle from the TMPA (a) is compared with those of seasonal precipitation forecasts from (b) CCM3, (c) NCEP, (d) NCAR, (e) NRL, and (f) MIT. The horizontal resolution is T63 ( $\sim 1.875^\circ$ ). Area averaged ( $50^\circ\text{S}$ - $50^\circ\text{N}$ ) values (first: land and ocean, second: land only, third: ocean only) are shown in the upper right corner.

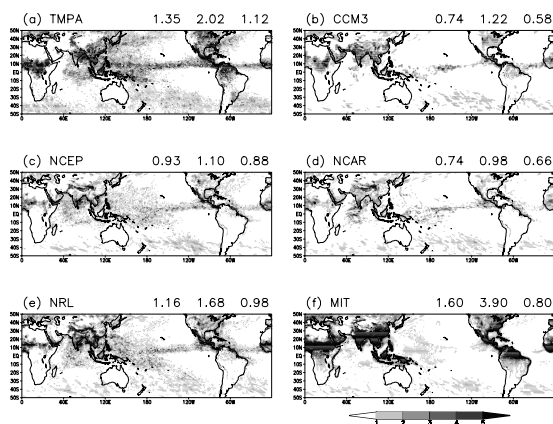


Fig. 2: As in Fig. 1, but for the T255 ( $\sim 0.469^\circ$ ) horizontal resolution. The resolution of CCM3 is T126 ( $\sim 0.938^\circ$ ).

### Acknowledgements

Computations were performed on the IBM SP4 at the FSU. COAPS receives its base support from the Applied Research Center, funded by NOAA Office of Global Programs awarded to Dr. James J. O'Brien.

### References

- Cocke, S., and T. E. LaRow, 2000: Seasonal predictions using a regional spectral model embedded within a coupled ocean-atmosphere model. *Mon. Weather Rev.*, **128**, 689-708.
- Huffman, G. J., R. F. Adler, D. T. Bolvin, G. Gu, E. J. Nelkin, K. P. Bowman, Y. Hong, E. F. Stocker, and D. B. Wolff, 2007: The TRMM Multisatellite Precipitation Analysis (TMPA): Quasi-global, multiyear, combined-sensor precipitation estimates at fine scales. *J. Hydrometeor.*, in press.

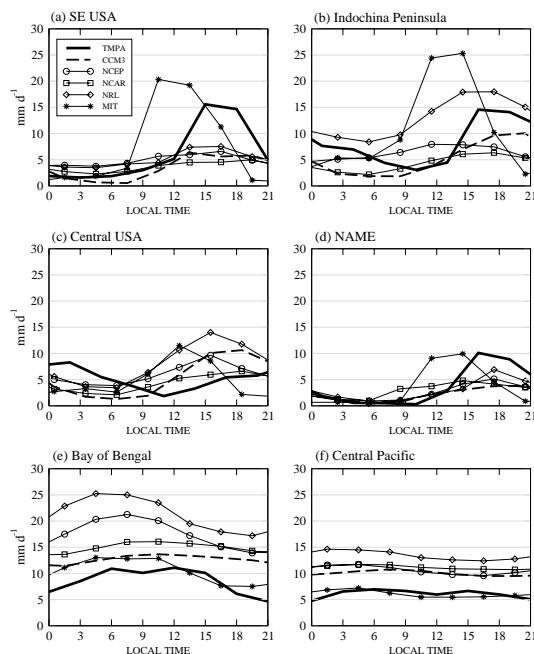


Fig. 3: Diurnal cycles of area-averaged precipitation amount ( $\text{mm d}^{-1}$ ) at six different regions. The abscissa is LST. The regions examined are (a) the southeast United States ( $25^\circ\text{N}$ - $35^\circ\text{N}$ ,  $90^\circ\text{W}$ - $75^\circ\text{W}$ ), (b) Indochina Peninsula ( $10^\circ\text{N}$ - $20^\circ\text{N}$ ,  $95^\circ$ - $110^\circ\text{E}$ ), (c) the central United States ( $35^\circ\text{N}$ - $44^\circ\text{N}$ ,  $100^\circ\text{W}$ - $90^\circ\text{W}$ ), (d) the North American Monsoon Experiment area ( $20^\circ\text{N}$ - $35^\circ\text{N}$ ,  $115^\circ\text{W}$ - $105^\circ\text{W}$ ), (e) Bay of Bengal ( $10^\circ\text{N}$ - $25^\circ\text{N}$ ,  $80^\circ$ - $95^\circ\text{E}$ ), and (f) the central Tropical Pacific ( $0^\circ$ - $10^\circ\text{N}$ ,  $180^\circ$ - $120^\circ\text{W}$ ).